UNIVERSIDAD NACIONAL DE COLOMBIA
SEDE MEDELLÍN
FACULTAD DE MINAS

DYNA
http://dyna.medellin.unal.edu.co/

Cr/CrN bilayer coating behavior under erosion-corrosion degradation by jet impingement testing

Johanna Alegría-Ortega [a], Luz Marina Ocampo-Carmona [a], Fernando Rodríguez [b] & Elena Forlerer [b]

[a] *Grupo de Ciencia y Tecnología de Materiales, Facultad de Minas, Universidad Nacional de Colombia, Medellín, Colombia. jaalegri@unal.edu.co*
[b] *Laboratorio de Recubrimientos y Tribología, Gerencia de Materiales, Comisión Nacional de Energía Atómica, Buenos Aires, Argentina. forlelrer@cnea.gov.ar*

Received: July 29th, 2015. Received in revised form: November 19th, 2015. Accepted: December 10th, 2015

Abstract
Cathodic arc technique was used to deposit a Cr/CrN bilayer coating on AISI 440C stainless steel. The morphology and composition of the coating were verified by Scanning Electron Microscope and X-Ray Diffraction. Hardness and adhesion of the coating were also studied. In the erosion-corrosion wear, a slurry jet with impingement angle 90° at 4 and 8 m/s was used to impact upon bare and coated steel. All the wear mechanisms were evaluated according to ASTM G-119.
The results indicate that the synergism wear rate is the most aggressive wear component, exceeding 40% of the total mass loss for coating steel and 60% of mass loss for bare steel. An increase in the impact velocity increases mass loss for both bare and coated steel. In comparison, the Cr/CrN coating had better corrosion and erosion–corrosion resistance.

Keywords: Multilayer coating, Staintess Steel, Cathodic Arc, erosion-corrosion.

Comportamiento de un recubrimiento bicapa de Cr/CrN bajo degradación por erosión-corrosión por ensayo de impacto con chorro

Resumen
La técnica de deposición catódica fue utilizada para depositar un recubrimiento bicapa de Cr/CrN sobre acero AISI 440C. La morfología y composición del recubrimiento fueron evaluadas con microscopía electrónica de barrido y difracción de rayos-x. La dureza y adhesión del recubrimiento también fueron estudiadas.
Se siguió el procedimiento de la norma ASTM G-119 para evaluar el desgaste por erosión-corrosión usando un chorro de lodo impactando a 90° a una velocidad de 4 y 8 m/s para impactar sobre el acero desnudo y recubierto.
Los resultados muestran que el sinergismo es la componente de desgaste más agresiva, ésta excede en un 40% la pérdida de masa total para el acero recubierto y el 60% de la pérdida de masa total para el acero desnudo. El incremento en la velocidad de impacto incrementa la pérdida de masa tanto en el acero desnudo como en el recubierto. Comparando, el recubrimiento de Cr/CrN presentó mayor resistencia a la corrosión y al desgaste por erosión–corrosión.

Palabras claves: Recubrimientos multicapas, Acero inoxidable, Arco catódico, erosión-corrosión.

1. Introduction

In aqueous conditions the presence of ions $(CO_3)^{2-}$, Cl^-, $SO_4^=$ and particles harder than the surface can cause rapid deterioration of metal parts, which could be mitigated by employing stainless steel or potentiostatic protection. However, a high flux of certain ions added with harder particles impacting the surface promote the breakdown of the protective layer.

Stainless steels and corrosion inhibitors enable the reduction of the mass loss associated with the pure corrosion effect, allowing erosion loss to be the principal component of wear, although their protective capacity lasts until the flow velocity and turbulence affect the integrity of the surface. Alternatively, ceramic coatings have been used because their

How to cite: Alegría-Ortega, J., Ocampo-Carmona, L.M., Rodríguez, F. and Forlerer, E., Cr/CrN bilayer coating behavior under erosion-corrosion degradation by jet impingement testing. DYNA 83(197), pp. 146-153, 2016.

high toughness and good adhesion can protect the surface against erosion, they could also extend the life of the part under corrosion due to their superior chemical resistance [1].

In general, erosion-corrosion (EC) studies reveal that the increase in the loss of material due to EC is greater than the sum of pure erosion and pure corrosion, which verifies the existence of a combined action [2-5]. It has also been found that for some metallic materials, the passivation zone promotes a decrease in the erosion rate, i.e. passive films generate some protection against erosive particles.

Stack et al. [3] suggest that under EC wear, wear rates are limited to four stages: corrosion stage 1, corrosion stage 2, increased wear by pure corrosion, and pure erosion. In the last stage, the effect is due to an increase in temperature and erosion velocity. For tests in which the mass loss is measured gravimetrically, corrosion stage 1 is characterized by mass loss associated with the dissolution or degradation of the natural protective Cr_2O_3 oxide; corrosion stage 2 shows a mass gain due to the formation of new oxides; in the increased wear by pure corrosion and pure erosion stages, the mass losses are more pronounced, due to the convective and diffusive flow action and the kinetic energy of the particles impinging on the surface, causing the generation of subsurface cracks. In order to decrease the mass loss rate due to stages 3 and 4, the deposition of ceramic coatings has been proposed as an alternative because of their high hardness, and their chemical and thermal inertia, which generate lower mass loss rates [1,5-6].

According to ASTM G-119 [2] the mass loss rate by E/C in aqueous media is described by the eq. (1):

$$TML = E_0 + C_0 + S \quad (1)$$

In which, TML: total mass loss rate, E_0: Mass loss rate by pure erosion, C_0: Mass loss rate by pure corrosion and S: erosion-corrosion synergism.

The synergism component can be seen as the sum of the interactions between the processes, where ΔC_w that is the change in corrosion rate due to wear and ΔW_c is the change in wear rate due to corrosion as is described by eq. (2):

$$TML = E_0 + C_0 + \Delta E_C + \Delta C_W \quad (2)$$

The additive effect, ΔCw, refers to the change in corrosion rate due to wear, a positive additive effect are related with the generation of rugosity, these stressed zones behave like electrochemical cells increasing material loss; when a negative additive effect occurs it means there are compressive stresses due to the impact of the erosive particles, this stress state alters the surface electrochemical behavior triggering a lower mass loss rate [3-6].

The synergistic effect, ΔWc, refers to the enhancement of wear due to corrosion, when this term is negative (antagonism) the corrosion products during wear are providing protection to the surface.

With PVD techniques, there has been success in obtaining coatings at low temperatures (below 400°C), high deposition rates, and the possibility to deposit multilayers or super-networks that exhibit better performance due to the combination of the properties of their components and the laminated structure [7-10]. Indeed, with the diversity of techniques that have emerged for the deposition of hard films, currently there are EC wear studies being carried out on various nitrides and carbides of transition elements, as well as on micro and nanometric multilayers of these, in order to propose better alternatives for the mitigation of the wear of metallic parts [5,6,11-13].

2. Materials and methods

The experimental procedure used can be divided into two steps: coating deposition and evaluation of coating performance under erosion-corrosion experiments.

The first step can be described as follows: Heat treatment of the steel, substrate characterization, coating deposition. The details of each stage will be presented below.

2.1. Heat treatment of AISI 440C steel

Samples of AISI 440C of 12.7 mm in diameter and 5 mm in thickness were subjected to cryo-quenching and tempering treatments (Fig. 1) in the Coatings and Tribology Laboratory (DRyT) of CNEA, to improve hardness and wear resistance. A cryo-quenching process was employed in order to reduce the retained austenite [14], which is metastable at room temperature and could transform to new martensite during quenching after coating, resulting in volume change, which generates internal stresses, and consequently unacceptable dimensional changes and delayed cracking [15,16].

2.2. Coating deposition

The samples were polished with abrasive paper from 80-800 mesh size. Some of the samples were used for the deposition of coatings and other bare samples were used as a reference for erosion-corrosion tests.

Two bilayers of Cr/CrN were deposited with cathodic arc equipment Nissin Electric CO, LTD RMP-R3-J, in the Coatings and Tribology Laboratory (DRyT) of CNEA.
For the deposition of the coatings, the vacuum back-pressure was $3x10^{-5}$ Torr ($4x10^{-3}$ Pa) using a two-stage rotative mechanical pump for the rough vacuum, coupled with a diffusion pump. The target-substrate working distance was

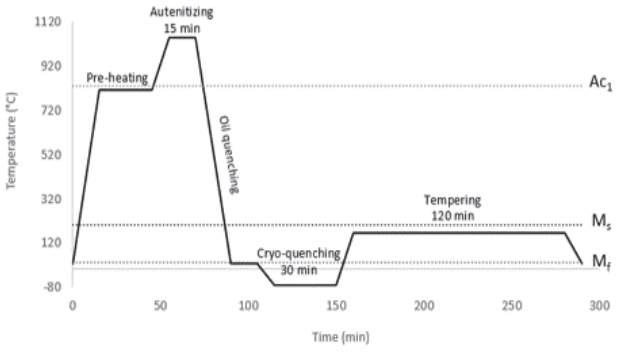

Figure 1 Heat Treatment of AISI 440C steel. Ac1: initiation of austenite transformation temperature, Ms: initiation of martensitic transformation temperature start, Mf: end of martensitic transformation temperature.
Source: The authors.

15 cm. The ionic cleaning was made with Vbias: -800V with Ar gas for 15 min. Then, the deposition of two bilayers of Cr + CrN, each layer under Vbias: -400V for 1.5 min with a flow rate of 40 cm^3 of Ar gas in the Cr layer deposition and Vbias: -125V for 15 min with a mixture of N_2 (36 cm^3) and Ar (2 cm^3) gases in the CrN layer deposition, was carried out. Between the two bilayers, the voltage sources were turned off without breaking the vacuum.

2.3. Evaluation of coating performance under erosion-corrosion experiments

The jet impingement test was executed in a cell that holds 5 L of solution and it was recirculated by means of a peristaltic pump. The nozzle is made of Nylon and has an outlet diameter of 2 mm, at 90° from the sample.

The cell, Fig. 2, was coupled to a potentiostat Gamry 600 to generate potentiodynamic polarization curves in order to evaluate the corrosion rate. The reference electrode (RE) of saturated calomel (SCE) was put into a glass shell with a Vycor tip, which acts as a membrane and facilitates electrochemical measurements without any contamination of the electrode. The auxiliary electrode (AE) of platinum was located near the working electrode (sample), to reduce the ohmic drop during the measurement.

Potentiodynamic curves were initiated once the open circuit potential (OCP) was stabilized. The exposure area of the sample was 78.54 mm^2. A sweep was carried out from -0.6 to 0.6 V vs SCE using a scan rate of 1 mV/s. In all the tests, the samples were immersed for 30 min in the solution or in the slurry under the action of the jet. The electrochemical parameters were calculated with Tafel extrapolation using E-Chem Analysis-Gamry software.

The corrosion tests were performed in a 3.5%wt. NaCl solution, while in the erosion and EC tests slurry composed of a solution with 10% wt. of silica particles of 0.300-0.212 mm (AFS 50/70) size was used. In the erosion test, a cathodic voltage of -1V vs E_{corr} was supplied in order to avoid mass loss associated with corrosion. In the slurry tests, a paddle stirrer was used in order to facilitate the suspension of the silica particles and supply a homogeneous solution to the pump.

The jet impingement velocities were 4 and 8 m/s. The test was performed at room temperature (25-28°C). The Nylon sample holder was of the Avesta cell type in order to avoid crevice corrosion. The sample was placed 5 mm from the nozzle. The mass loss erosion and EC test were calculated gravimetrically.

The nomenclature used in the samples was as follows: Table 1.

Table 1.
Nomenclature used for corrosion-erosion test.

Material type	Test type	Impact velocity
a: 440C steel	**TML:** Total material loss by erosion-corrosion	**4**: 4m/s
R: Cr/CrN Bilayer coating	**W_0:** pure erosion **C_0:** pure corrosion **C_w:** electrochemical corrosion rate during the erosion – corrosion test	**8**: 8m/s

Source: The authors.

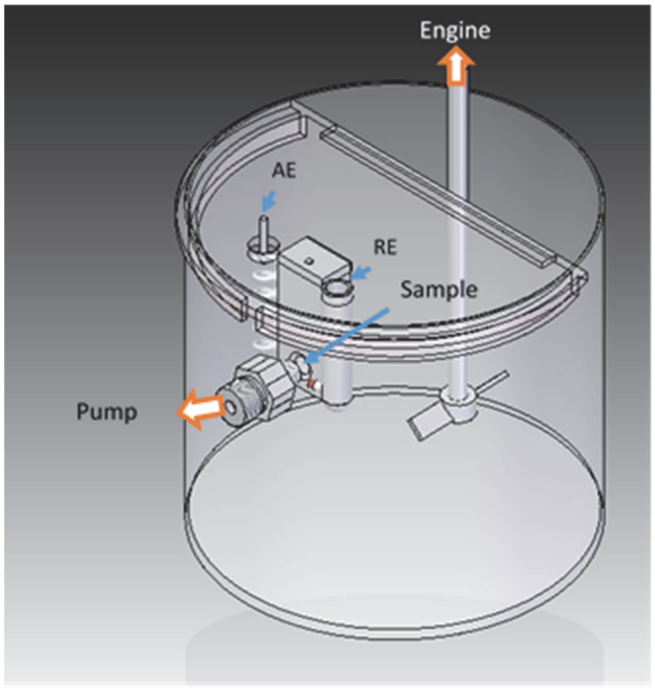

Figure 2 Erosion corrosion cell.
Source: The authors.

3. Results and Discussion

The characterization of the substrates after the heat treatment, the coating and the electrochemical measurements of mass loss of the coated and uncoated samples after completing the tests, as well micrographs will be reported.

3.1. Characterization of substrates

The monograph in Fig. 3 shows that the steel was etched with Beraha attack [17] and that there is a dark matrix consistent with very fine martensitic matrix exhibited by

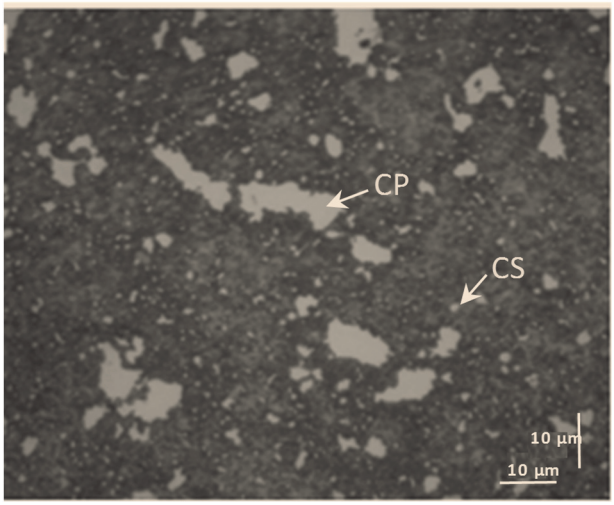

Figure 3 Bright field micrograph of 440C steel after cryo-quenching and tempering treatment. CP: primary carbides, CS: secondary carbides. Etched with Beraha.
Source: The authors.

440C steel thermal treated [18], and bimodal size distribution of white areas, which correspond to carbides. A martensitic matrix was checked by measuring the microhardness, by means of a microdurometer Akashi MVK-H2, which gave a result of (679 ± 71) HV0.025.

3.2. Coating characterization

The evaluation of the properties of the coating was performed on a standard sample for each batch of coatings, using the equipment of the CTL-CNEA.

The hardness measurement was (1300 ± 80) HV0.025. Fig. 4 shows a micrograph of thickness coating measured with CaloTest equipment CSEM S/N 03-134. The partial and full thickness measured was 3,2 µm and 6,6 µm respectively.

The scratch test was performed with CSEM Scratch-Tester S-N 26-393 equipment with a diamond type C Rockwell indenter. The indenter was moved at a speed of 10 mm/min, linearly varying the load from 0 to 60 N with a table speed of 100 N/mm. The critical load was determined by optical microscope, and the lineal relation of load vs. table speed was Lc_1: (38 ± 10) N.

To identify the phases present and their preferred orientation, diffraction measurements were performed on an X-ray diffractometer X'pert Panalytical with Cu-Kα radiation. The diffraction pattern, Fig. 5, shows the presence of a CrN phase (JCPDF00-011-0065). It can be noticed that the film has a strong texture at CrN [220] orientation. This is consistent with the information presented by many authors [19-22] for the combination of parameters used in the deposition of this coating, since the texture of the films is affected by the Vbias and nitrogen partial pressure used in the deposition process [19-21]. The Cr peaks have shifted to the left indicating that the crystalline structure has compression microstresses that help to counteract subsurface tangential stresses during erosion preventing pitting and chipping of the coating. Microstresses alter the lattice spacing and broadening the diffraction peak [23]. It does not present evidence of Cr peaks.

Fig. 6a shows the surface microstructure of the coating, in which some surface defects like pinholes and droplets,

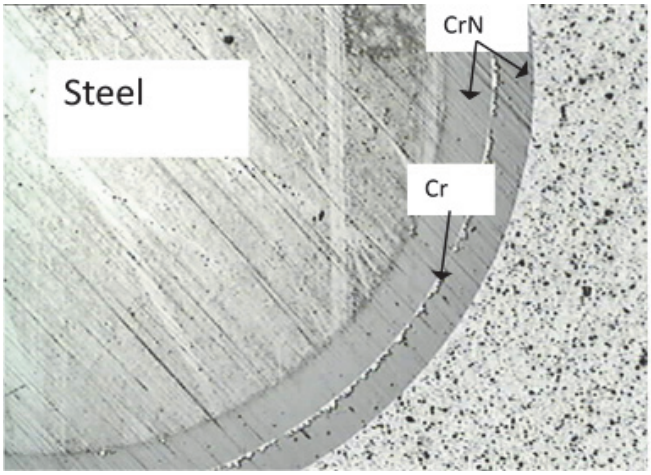

Figure 4 Optical micrograph at 50X of ball crater thickness test for Cr/CrN bilayer coating.
Source: The authors.

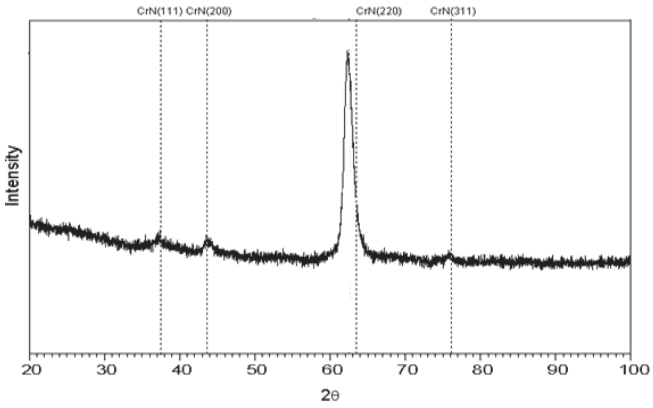

Figure 5 Diffractogram of Cr/CrN coating on AISI 440C steel.
Source: The authors.

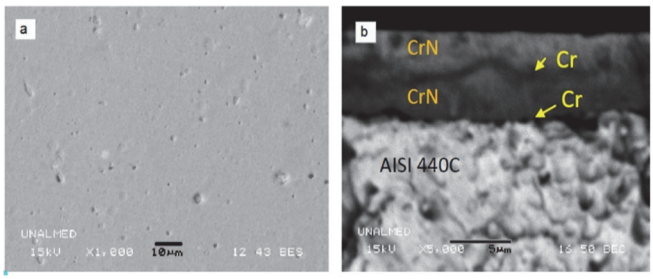

Figure 6 SEM micrographs of Cr/CrN coating. a) Surface. b) Transversal.
Source: The authors.

characteristic of process deposition, are seen. The micrographs were performed with SEM *JEOL* JSM 5910 LV at UNal laboratories.

Fig. 6b is a transversal micrograph of the coating, and it was obtained by previously fracturing a sample immersed in liquid nitrogen and etching the multilayer coating with a solution of HNO_3 and HF in the ratio 1:9 for 30 min. This preferentially attacks the Cr, and so can display the stratification layers.

3.3. Electrochemical measurements

The polarization curves for pure corrosion (C_0) and erosion-corrosion (C_w) carried out on 440C steel and on a Cr/CrN bilayer coating in function of the impact velocity are shown in Fig. 7.

For all conditions of wear, the velocity increase causes a higher corrosion current density. Although the corrosion potential of coated samples are very close to bare samples, coating protects the surface under conditions of pure corrosion as well as EC, as is observed in Fig. 7, since corrosion current density is lower for coated samples.

3.4. Mass losses

Table 2 shows the individual contributions of erosion, corrosion and synergism for each of the evaluated conditions obtained, following the procedure described in ASTM G-119-09 [2]. Generally, increasing the velocity produces a

(a)

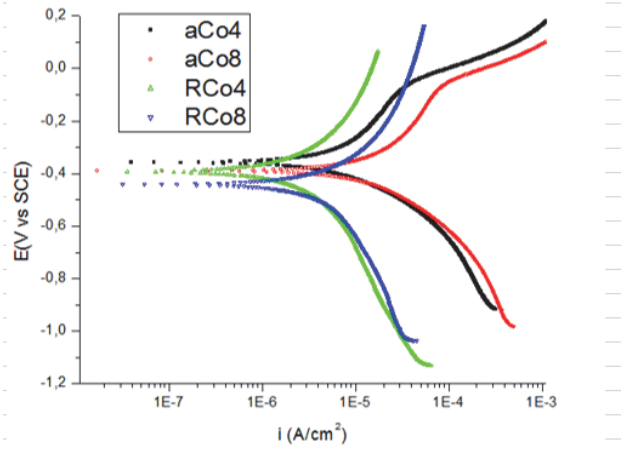

	aCo4	aCo8	RCo4	RCo8
i corr (A/cm²)	1,48 e-6	5,26 e-6	5,39 e-7	1,03 e-6

(b)

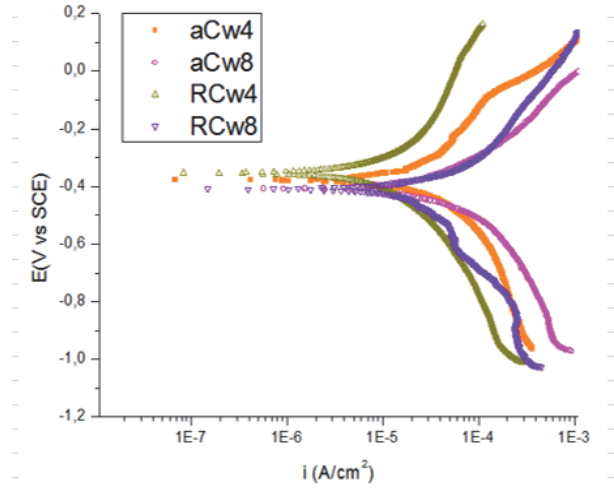

	aCw4	aCw8	RCw4	RCw8
i corr (A/cm²)	1,26 e-7	2,69 e-7	1,60 e-6	1,58 e-5

Figure 7. Potentiodynamic polarization curves made at different velocities on the 440C steel and the coating of Cr/CrN in a) pure corrosion b) erosion-corrosion.
Source: The authors.

higher mass loss rate, which is in accordance with the theories of erosion. Also, it should be noted that there is a greater loss of mass for both materials in erosion-corrosion conditions, the case of martensitic stainless steel being more drastic.

The pure corrosion mechanism (C_0) has little effect on the coating and on stainless steel under any of the test conditions. The pure erosion mechanism (W_0) was the greatest wear mechanism, mass loss being higher for uncoated steel. The protective effect of the coating for pure erosion decreases with increasing impact velocity. Moreover, the synergism effect in erosion-corrosion is remarkable for all other conditions, and even more so for the uncoated samples (TML). Under the conditions tested and with the values reported in Table 2, Fig. 8 shows the percentage contribution of mass loss; for both the CrN/Cr coating as well as the 440C steel the synergism exceeds 40% of the total mass loss, which means that the mechanisms of interaction between erosion and corrosion are very important for the wearing down of both materials. For all conditions, the coating had a higher resistance, represented by a mass loss rate of about half compared with that obtained for the bare 440C steel. Fig. 9 shows the SEM micrographs, which confirm that the Cr/CrN bilayer coating exposed to pure erosion undergoes less material detachment at low velocity, without any observable EDS peaks from the substrate. For the eroded surfaces under EC, Fig. 9c and d, the material detachment is greater and a large and deep scar area in the center of the samples can be seen. Debris were observed scattered around the scar coating. In Fig. 9d, for high velocity EC it can be observed that there is a degradation of the substrate, which shows plastic deformation with the formation of valleys generated by the impact of the particles as observed in metals like aluminum. The direction range of valleys comes from the interaction between the particles in the jet due to their high concentration, which generates changes in the trajectories, which is reinforced by the particle size distribution in the jet [24]. The EDS of Fig. 9d was taken in the central zone of the sample, it shows Fe peaks and due to the height of the Fe/Cr peaks is close to that typical of bare steel, it seems that the substrate surface has been uncovered. Therefore, it can be confirmed that the fracture toughness and hardness of the coating is critical for erosion resistance, since the coating has a mode of failure by brittle fracture. For all cases, the synergistic effect (ΔW_c) is positive, being of a higher value for bare steel. This situation suggests that the surface does not produce corrosion products that help protect the surface [2-4, 25-26], which is confirmed in the potentiodynamic polarization curves of corrosive flux particles, which are shown in Fig. 6. It can be seen that there is no characteristic curve with anodic formation of passive layers. The coating was also unable to produce corrosion products that protect the surface, but the ΔWc data are less positive, which provides protection twice that of 440C stainless steel.

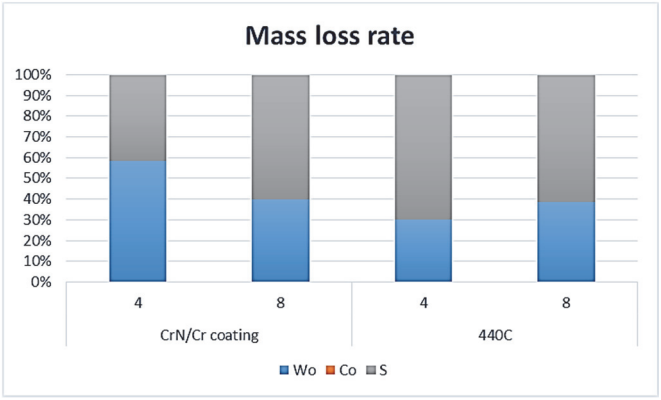

Figure 8 Percentage contribution of pure erosion, pure corrosion and synergism over total mass loss rate by erosion-corrosion wear.
Source: The authors.

Table 2.
Mass loss rate in the EC test. TML: Total material loss rate; W_0: mechanical wear rate; C_0: electrochemical corrosion rate; C_w: electrochemical corrosion rate during the corrosive wear process; S: Synernism; ΔW_c: Synergistic effect; ΔC_w: Additive effect.

Sample material		CrN/Cr coating		440C	
Impact velocity (m/s)		4	8	4	8
Mass loss rate (mm/ year)	TML	9,3728	15,6213	28,4530	36,9889
	W_o	5,4674	6,2485	8,5359	14,2265
	C_o	6,8910E-06	1,3214E-05	1,7179E-05	6,1240E-05
	S	3,9053	9,3727	19,9171	22,7623
	ΔCw	1,3513E-05	1,8903E-04	1,0905E-04	2,0800E-04
	ΔWc	3,9053	9,3726	19,9170	22,7621

Source: The authors.

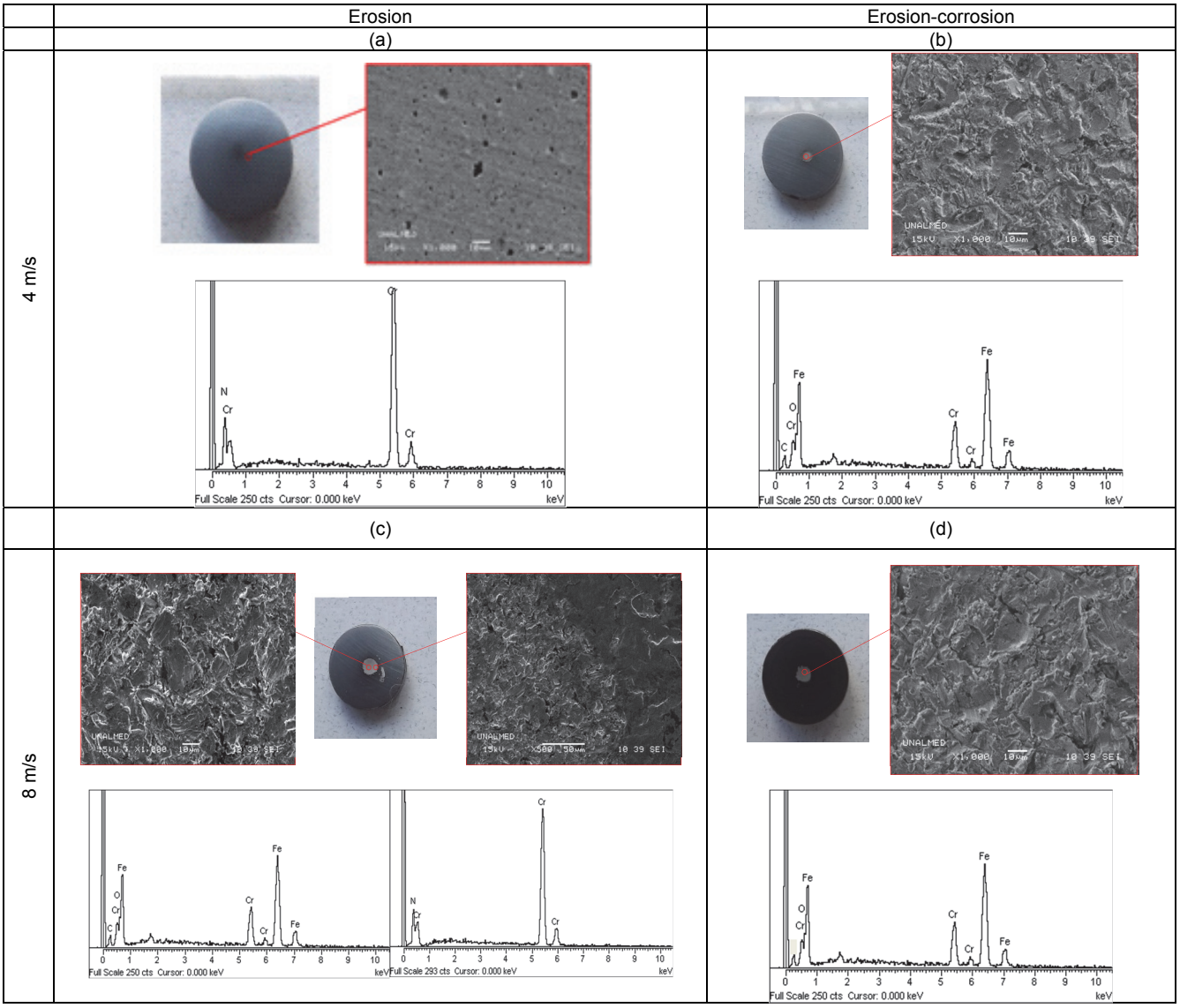

Figure 9. SEM micrographs of coatings after pure erosion and erosion-corrosion tests.
Source: The authors.

Different authors [5-6,11-13], who have studied some alloys and coatings, reported that synergism is an important component of the degradation in EC. Synergism in the case of alloys that undergo passivation is linked to the breakdown of the passive film by the action of the particles. For the case of multiple layers, as in the case of ceramic coatings, the EC mechanisms and the synergism may be more complex, due to the presence of galvanic between Cr and Fe.

4. Conclusions

The bilayer coating of Cr/CrN offered resistance to erosion, corrosion and erosion-corrosion under the impact of 4 to 8 m/s compared to the bare surface.

The corrosion potential of potentiodynamic polarization curves is very similar to the bare surface, which can be attributed to the electrolyte penetrating the porosity of the coating.

Under the action of jet impact with slurry at 8 m/s, the coating fractured and detached from the substrate. Hence it is recommended that the adhesion of the coating be increased in order to prevent detachment, and also to heat treat the coating after processing in order to achieve a better toughness.

The pure corrosion rate compared to pure erosion is negligible, due to the high solid content (10% wt.) in the case of erosion, which generates a greater amount of impact, causing greater wear on surfaces through the mechanical effect.

At higher impact velocity, mass loss increased in terms of erosion, flow corrosion and EC for both materials (440C steel, bare and with coating).

The EC wear for all conditions tested was higher than the sum of the rates of pure erosion and pure corrosion, except for the case of steel subjected to erosion at 4 m/s.

It was possible to establish that the synergism exceeds 40% of the mass loss for all cases tested, and therefore is an important component of low mass loss under EC wear.

The 440C steel surface showed a mass loss rate of 304% under an impact of 4 m/s and 237% under an impact of 8 m/s compared to the coating mass loss rates.

Acknowledgments

The authors would like to thank Hugo Estupiñan, Ph.D., for his assistance in the electrochemical measurements. We are grateful to the Argentine Atomic Energy Commission (CNEA) and the National University of Colombia (UNal) for the use of the equipment and the laboratories, at CNEA (Coatings and Tribology Laboratory, metallography, X-ray diffraction) and at UNal (metallography laboratories and testing of materials, advanced microscopy). Thanks go to Dr. Norma Mingolo (CNEA), Mery Arrubla, Martin Griffiths (CNEA) and Manuel Iribarren (CNEA), for their help in conducting the tests, and to COLCIENCIAS and the Directorate of Research, National University of Colombia-Medellín (DIME) for the financial support given through the notice of Opening for Young Researchers No. 510 (2010).

References

[1] Mattox, D.M., Handbook of physical vapor deposition (PVD) processing: film formation Adhesion, Surface Preparation and Contamination Control (Materials Science and Process Technology). USA: Noyes Publication, 1998. DOI: 10.1016/B978-081551422-0.50010-3

[2] ASTM G119-09, Standard guide for determining synergism between wear and corrosion. ASTM International, West Conshohocken, PA, 2003, DOI: 10.1520/G0119-09. DOI: 10.1520/G0119-09

[3] Stack, M.M., Lekatos, S. and Stott, F.H., Erosion-corrosion regimes: Number, nomenclature and justification? Tribology International, 28, pp. 445-451, 1995. DOI: 10.1016/0301-679X(95)00009-S

[4] Stack, M.M., Zhou, S. and Newman, R.C., Identification of transitions in erosion-corrosion regimes in aqueous environments. Wear, 186-187, pp. 523-532, 1995. DOI: 10.1016/0043-1648(95)07175-X

[5] Stack, M.M. and Wang, W.H., The slurry erosive wear of physically vapour deposited TiN and CrN coatings under controlled corrosion. Tribology Letters, 6, pp. 23-36, 1999. DOI: 10.1023/A:1019186918225

[6] Stack, M.M. and Wang, H.W., Simplifying the erosion–corrosion mechanism map for erosion of thin coatings in aqueous slurries. Wear, 233, pp. 542-551, 1999. DOI: 10.1016/S0043-1648(99)00216-1

[7] Kot, M., Rakowski, W.A., Major, Ł., Major, R. and Morgiel, J., Effect of bilayer period on properties of Cr/CrN multilayer coatings produced by laser ablation. Surface & Coatings Technology, 202, pp. 3501-3506, 2008. DOI: 10.1016/j.surfcoat.2007.12.036

[8] Kaciulis. S., Mezzi, A., Montesperelli, G., Lamastra, F., Rapone, M., Casadei, F., Valente, T. and Gusmano, G., Multi-technique study of corrosion resistant CrN/Cr/CrN and CrN:C coatings. Surface & Coatings Technology, 201, pp. 313-319, 2006. DOI: 10.1016/j.surfcoat.2005.11.128

[9] Marulanda, D.M., Olaya, J.J., Piratoba, U., Mariño, A. and Camps, E., The effect of bilayer period and degree of unbalancing on magnetron sputtered Cr/CrN nano-multilayer wear and corrosion. Thin Solid Films, 519, pp. 1886-1893, 2011. DOI: 10.1016/j.tsf.2010.10.010

[10] Aperador, W., Ramírez, C. and Caicedo, J.C., The effect of Ti(CN)/TiNb(CN) coating on erosion-corrosion resistance. Ingeniería e Investigación, 32(2), pp. 6-11, 2012.

[11] Purandare, Y., Stack, M.M. and Hovsepian, P., Velocity effects of erosion-corrosion of CrN/Nb superlattice PVD coatings. Surface & Coatings Technology, 201, pp. 361-370, 2006. DOI: 10.1016/j.surfcoat.2005.11.143

[12] López, D., Sanchez, C. and Toro, A., Corrosion-Erosion behavior of TiN-coated stainless steels in aqueous slurries. Wear, 258, pp. 684-692, 2005. DOI: 10.1016/j.wear.2004.09.015

[13] López, D., Congote, J.P., Cano, J.R., Toro, A. and Tschiptschin, A.P., Effect of particle velocity and impact angle on the corrosion–erosion of AISI 304 and AISI 420 stainless steels. Wear, 259, pp. 118-12, 2005. DOI: 10.1016/j.wear.2005.02.032

[14] Barlow, L., The effect of austenitising and tempering parameters on the microstructure and hardness of martensitic stainless steel AISI 420. MSc. Thesis. University of Pretoria. Pretoria, South Africa, 2009.

[15] Das, D., Dutta, A.K. and Ray, K.K., Influence of varied cryotreatment on the wear behavior of AISI D2 steel. Wear, 266, pp. 297-309, 2009. DOI: 10.1016/j.wear.2008.07.001

[16] Jha, A.K., Swathi-Kiranmayee, M., Ramesh-Narayanan, P., Sreekumar, K. and Sinha, P.P. Metallurgical analysis of ball bearing seized during operation. Journal of Materials Engineering and Performance, 21, pp. 1076-1084, 2012.

[17] Vander-Voort, G.F., Manilova, E.P., Michael, J.R. and Lucas, G.M., Study of selective etching of carbides in steel. www.dgm.de. Buehler Ltd. [Online]. [date of reference September 16th of 2013]. Available at: <www.dgm.de/past/2004/metallographie/download/686-60.pdf>

[18] ASM Handbook., Vol. 4. Heat Treatment. USA, 1991.

[19] Grant, W.K., Loomis, C., Moore, J.J., Olson, D.L., Mishra, B. and Perry, A.J., Characterization of hard chromium nitride coatings deposited by cathodic arc vapor deposition. Surface and Coatings Technology, 86-87, pp. 788-796, 1996. DOI: 10.1016/S0257-8972(96)03071-X

[20] Oden, M., Ericsson, C., Håkansson, G. and Ljungcrantz, H., Microstructure and mechanical behavior of arc-evaporated Cr–N coatings. Surface and Coatings Technology, 114, pp. 39-51, 1999. DOI: 10.1016/S0257-8972(99)00019-5

[21] Ahn, S.H., Choi, Y.S., Kim, J.G. and Han, J.G., A study on corrosion resistance characteristics of PVD Cr-N coated steels by electrochemical method. Surface and Coatings Technology, 150, pp. 319-326, 2002. DOI: 10.1016/S0257-8972(01)01529-8

[22] Chipatecua-Godoy Y.L., Marulanda-Cardona D.M. and Olaya-Flórez J.J., Evaluating the corrosion resistance of UBM-deposited Cr/CrN multilayers. Ingeniería e Investigación, 31(1), pp. 16-25, 2011.
[23] Noyan, C. and Cohen, J.B., Residual stresses - Measurement by diffraction and Interpretation. USA: Springer-Verlag, 1987.
[24] Efird, K.D., Jet impingement testing for flow accelerated corrosion. Corrosion 2000. NACE International, 2000.
[25] Chang, Z.K., Wan, X.S., Pei, Z.L., Gong, J. and Sun, C., Microstructure and mechanical properties of CrN coating deposited by arc ion plating on Ti6Al4V substrate. Surface & Coatings Technology, 205, pp. 4690-4696, 2011. DOI: 10.1016/j.surfcoat.2011.04.037
[26] Warcholinski, B. and Gilewicz, A., Tribological properties of CrNx coatings. Journal of Achievements in Materials and Manufacturing Engineering. 37, pp. 498-504, 2009.

J. Alegría-Ortega, received her BSc. in Mechanical Engineering in 2009 and her MSc. degree in Materials and Manufacture Process in 2012, both from the Universidad Nacional de Colombia. Medellin, Colombia. From 2008 to 2011, she worked as quality management system coordinator in a Materials Laboratory of Universidad Nacional de Colombia. Medellin, Colombia. Currently, she is working as a project engineer in a consulting engineering company.
ORCID: 0000-0002-2934-5470

L.M. Ocampo-Carmona, received her BSc. in Chemical Engineering in 1994, her MSc degree in Metallurgical and Materials Engineering in 2000, and a Dr. degree in Metallurgical and Materials Engineering in 2005, all from the Universidade Federal do Rio de Janeiro, Rio de Janeiro, Brazil. She worked as a teacher in chemistry, fluid mechanics, and strength of materials in the Universidad de Antioquia from 1996 to 1998. She is a full professor since 2006 in Department of Materials and Minerals, Facultad de Minas, Universidad Nacional de Colombia, Medellin, Colombia. She teaches chemistry metallurgy, physical metallurgy, metallurgical electrochemistry, electrometallurgy and corrosion, and materials science at undergraduate level and Fundamentals of corrosion at the Masters and Doctorate level. Her research interests include Corrosion and protection of metals, recycling of materials, bio-materials, and electrochemistry.
ORCID: 0000-0002-8117-1391.

F.M. Rodríguez, is Technician in 1978. He started working for the National Atomic Energy Commission, Argentina in 1984 and was involved in Vacuum technology projects and in Plasma coatings in 1997. He obtained a plasma materials process specialization in Nagoya University, Japan in 1997. He has been involved in the Arc-PVD process for more than 15 years.
ORCID: 0000-0001-9952-2420

E. Forlerer, received her BSc in Physical Science in 1976 and a PhD. in 1994 in Physics, from the Universidad Nacional de Buenos Aires, Argentina. She taught materials science at the Instituto Sabato of the Universidad Nacional de San Martin between 1994-2004 at the MSc. degree level. Since 2001, she has been Master's thesis and Doctoral advisor in materials science. She is currently Head of the Coatings and Tribology Laboratory at the Argentine National Atomic Energy Commission. Currently, her research is focused on thin film coatings as barriers for corrosion, wear, thermal transference, and diffusion.
ORCID: 0000-0003-3309-4544.